Can. J. Remote Sensing, Vol. 31, No. 2, pp. 191–206, 2005

Vegetation class dependent errors in lidar ground elevation and canopy height estimates in a boreal wetland environment

Chris Hopkinson, Laura E. Chasmer, Gabor Sass, Irena F. Creed, Michael Sitar, William Kalbfleisch, and Paul Treitz

Abstract. An airborne scanning light detection and ranging (lidar) survey using a discrete pulse return airborne laser terrain mapper (ALTM) was conducted over the Utikuma boreal wetland area of northern Alberta in August 2002. These data were analysed to quantify vegetation class dependent errors in lidar ground surface elevation and vegetation canopy surface height. The sensitivity of lidar-derived land-cover frictional parameters to these height errors was also investigated. Aquatic vegetation was associated with the largest error in lidar ground surface definition (+0.15 m, SD = 0.22, probability of no difference in height $P < 0.01$), likely a result of saturated ground conditions. The largest absolute errors in lidar canopy surface height were associated with tall vegetation classes; however, the largest relative errors were associated with low shrub (63%, –0.52 m, $P < 0.01$) and aquatic vegetation (54%, –0.24 m, $P < 0.01$) classes. The openness and orientation of vegetation foliage (i.e., minimal projection of horizontal area) were thought to enhance laser pulse canopy surface penetration in these two classes. Raster canopy height models (CHMs) underestimated field heights by between 3% (aspens and black spruce) and 64% (aquatic vegetation). Lidar canopy surface height errors led to hydraulic Darcy–Weisbach friction factor underestimates of 10%–49% for short (<2 m) vegetation classes and overestimates of 12%–41% for taller vegetation classes.

Résumé. Un relevé par capteur à balayage lidar aéroporté (« light detection and ranging ») utilisant un capteur cartographique laser aéroporté ALTM (« airborne laser terrain mapper ») basé sur les retours d'impulsions discrètes a été réalisé au-dessus du secteur de terres humides de Utikuma en zone boréale, au nord de l'Alberta, en août 2002. Ces données ont été analysées pour quantifier les erreurs reliées à la classe de végétation dans l'estimation lidar de l'élévation du terrain et de la hauteur du couvert de végétation. La sensibilité des paramètres de frottement du couvert dérivés par lidar à ces erreurs dans la hauteur a aussi été analysée. La végétation aquatique a été associée aux erreurs les plus grandes dans la définition lidar de la surface (+0.15 m, SD = 0.22, $P < 0.01$), dû probablement à la condition saturée de la surface. Les plus grandes erreurs absolues dans la hauteur lidar du couvert étaient associées aux classes de végétation haute. Toutefois, les erreurs relatives les plus grandes étaient associées à la classe caractérisée par des arbustes de faible taille (63 %, –0,52 m, $P < 0{,}01$) et à la végétation aquatique (54 %, –0,24 m, $P < 0{,}01$). L'ouverture et l'orientation du feuillage (i.e. la projection minimale de la surface horizontale) sembleraient faciliter la pénétration de l'impulsion laser à la surface du couvert dans ces deux classes. Les modèles matriciels de hauteur du couvert (CHM) ont sous-estimé la hauteur des champs d'une valeur variant entre 3 % (peupliers et épinettes noires) et 64 % (végétation aquatique). Les erreurs dans la hauteur lidar du couvert ont mené à des sous-estimations du facteur de frottement hydraulique de Darcy–Weisback d'une valeur variant entre 10 % et 49 %, dans le cas des classes de végétation basse (<2 m), et à des surestimations de 12 % à 41 %, pour les classes de végétation plus haute.
[Traduit par la Rédaction]

Introduction

The Western Boreal Plains (WBP) (**Figure 1**) is vulnerable to climate change (Schindler, 1997). Predictions indicate a warmer and drier climate that could alter the function and structure of this already water-stressed ecosystem (Winter and Rosenberry, 1998). The vulnerability of the WBP is amplified by land-use and land-cover changes caused by the extraction of natural resources (Schindler, 1998). Timber, oil, and gas extraction has resulted in the creation of thousands of kilometres of access roads and seismic corridor networks (Smith and Lee, 2000). To explore the effects of natural and

Received 3 December 2003. Accepted 10 December 2004.

C. Hopkinson,[1] L.E. Chasmer, and P. Treitz. Department of Geography, Queen's University, Kingston, ON K7L 3N6, Canada.
G. Sass and I.F. Creed.[2] Department of Geography, The University of Western Ontario, London, ON N6A 5C2, Canada.
M. Sitar and W. Kalbfleisch. Optech Incorporated, Toronto, ON M3J 2Z9, Canada.

[1]Corresponding author. Present address: Applied Geomatics Research Group, Centre of Geographic Sciences, NSCC Annapolis Valley Campus, 50 Elliot Road, R.R.1 Lawrencetown, NS B0S 1M0, Canada (e-mail: chris.hopkinson@nscc.ca).
[2]Present address: Department of Biology, The University of Western Ontario, London, ON N6A 5B6, Canada.

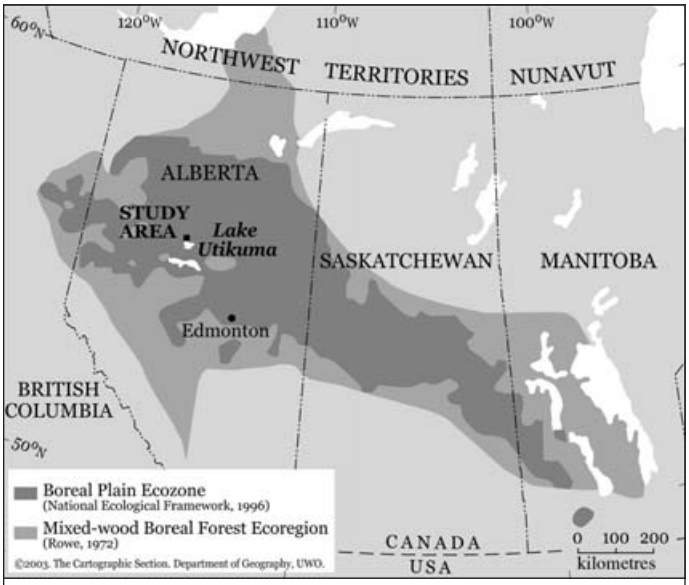

Figure 1. The Utikuma study area within the Western Boreal Plains of Canada.

anthropogenic stresses on the hydroecology of this region, a collaborative research project has been initiated entitled Hydrology, ecology, and disturbance (HEAD) of the western boreal wetlands (Devito et al., 2000). The focal point of the HEAD study is a hydrogeologic gradient located in the Utikuma Uplands, north of Utikuma Lake in Alberta, Canada. An airborne light detection and ranging (lidar) data-collection campaign was organised to produce a high-resolution ground digital elevation model (DEM_{ground}), a canopy digital elevation model (DEM_{canopy}), and a canopy height model (CHM) to be used in process-based energy-balance and hydrological models within the region.

With recent advances in laser and navigational technology, airborne scanning lidar is increasingly being used to collect ground surface elevation and vegetation height data, at submetre precision in three dimensions (Baltsavias, 1999). For an overview of lidar applications, the applicability of lidar to flood mapping, and the applicability of lidar to vegetation-height mapping, the reader is referred to Gutelius (1998), Heinzer et al. (2000), and St-Onge et al. (2003), respectively.

Models used to calculate land-cover energy fluxes have been shown to be sensitive to errors in vegetation parameterizations, and the need for accurate height estimates has been highlighted (Crawford and Bluestein, 2000; Schaudt and Dickinson, 2000). Roughness length calculations derived from profiling lidar estimates of vegetation height have been shown to agree well with field measurements over relatively arid grass and shrub-land areas (Menenti and Ritchie, 1994). In a similar study conducted by Weltz et al. (1994) there was some underestimation of canopy height, a result common to many scanning lidar studies (e.g., Magnussen et al., 1999; Gaveau and Hill, 2003). Underestimating canopy height is typically attributed to (*i*) laser pulse penetration into the foliage, (*ii*) insufficient representation of canopy apices due to low sample point density (St-Onge et al., 2003), or (*iii*) overestimation of ground height due to minimal pulse penetration through dense vegetation (e.g., Weltz et al., 1994; Reutebuch et al., 2003). Ground height biases of up to 0.2 m have been observed for wetland and riparian vegetation covers (Bowen and Waltermire, 2002; Töyrä et al., 2003), and these biases have been found to vary with land cover (Töyrä et al., 2003; Hodgson and Bresnahan, 2004).

Many studies have investigated the use of lidar for tree height measurement and found good relationships between lidar and field measures, with coefficient of determination values (r^2) typically ranging from 0.85 to 0.95 (Maclean and Krabill, 1986; Ritchie, 1995; Næsset, 1997; 2002; Magnussen and Boudewyn, 1998; Means et al., 2000; Witte et al., 2001; Næsset and Økland, 2002; Popescu et al., 2002; Lim et al., 2003a; 2003b). According to Davenport et al. (2000), short crop vegetation heights can be predicted from the standard deviation of lidar heights. This indirect height estimation approach has been used in various recent studies for floodplain friction parameterization (Cobby et al., 2001; 2003; Mason et al., 2003). These studies did not ascertain the level of error associated with directly measuring the canopy surface height for short (<2 m) vegetation, however. In addition, the approach used in these studies filters the data with a moving window to model vegetation heights and thus will tend to generate data of a lower resolution than that of the raw lidar data.

An important land-cover friction parameter used in hydrological models that can be estimated from vegetation height h is the Darcy–Weisbach friction factor f. This is a land-surface or channel-roughness coefficient often employed in hydrological models to enable the calculation of horizontal flow patterns, water levels, and velocity. Assuming similar rigidity, shape, and momentum absorbing area properties for a given vegetation class, f can be estimated as a function of height. For vegetation of height approximately >1 m, f can be considered inversely proportional to height (from Mason et al., 2003) as follows:

$$f = 4.06 \frac{V}{\sqrt{\xi E/\rho}} \frac{y}{h} \tag{1}$$

where V is the velocity, ξE is a vegetation elasticity term, ρ is the density of water, and y is the water depth. For submerged short vegetation (approximately <1 m), f can be related to a logarithmic function of height (Fathi-Maghadam and Kouwen, 1997; Kouwen and Fathi-Maghadam, 2000; Mason et al., 2003) as follows:

$$\frac{1}{\sqrt{f}} = a + b \log \left\{ \frac{y}{0.14h \left[\left(\frac{3.19h^{3.3}}{\tau} \right)^{0.25} \Big/ h \right]^{1.59}} \right\} \tag{2}$$

where a and b are fitted parameters related to the local boundary shear stress τ.

The objective of this paper is to evaluate the capability of airborne scanning lidar to directly measure vegetation canopy height for a range of common vegetation types within the WBP environment. The accuracy and systematic biases within the derived ground elevation and vegetation height data are quantified. This accuracy assessment is an essential step in the use of these data for subsequent hydrological, ecological, and energy-balance modeling efforts. The analysis presented is one of the first in-depth assessments of vegetation class dependent error in lidar estimates of ground height and vegetation canopy height and the subsequent sensitivity of land-cover friction parameter estimation using lidar CHM estimates.

Study area

The study was conducted in the Utikuma Uplands located north of Utikuma Lake, Alberta, Canada (**Figure 1**), along a 40 km × 6 km transect (**Figure 2**). The transect is representative of the hydrogeology within the region and contains a clay plain, a moraine, and a sand plain. Topography along the hydrogeologic gradient is subtle, with a relief of about 75 m. Vegetation is dictated by soil moisture conditions, with relatively dry sites dominated by trembling aspen (*Populus tremuloides* Michx.), very dry sites dominated by jack pine (*Pinus banksiana* Lamb.), and imperfectly drained peatland sites dominated by black spruce (*Picea mariana* Mill.). Hydrology is characterized by disintegrated surface drainage, with most horizontal flow terminating at the closest wetland. There are some rivers draining into Utikuma Lake, however, or draining out through Utikuma River, eventually emptying into the Peace River.

Field data collection

Airborne lidar survey

The study site DEM and sample locations are illustrated in **Figure 2**. The lidar survey was conducted on 28 August 2002, and the sensor used for the survey was an Optech Incorporated ALTM model 2050. The ALTM 2050 is a high-resolution, discrete dual pulse return (first and last), small footprint scanning lidar with manufacturer-quoted vertical and horizontal standard deviation accuracies of ±0.15 m and 1/2000 flying height, respectively. Optech Incorporated calibrated the sensor locally a week prior to data collection, and the calibration was checked again the following week.

The lidar survey adopted a narrow scan angle of ±16° from nadir, with approximately 50% swath overlap (200% total coverage). Twenty flight lines were surveyed in total. This increased the likelihood of obtaining laser pulse returns from the true ground surface over as much of the study area as possible and ensured that the average scan angle on the ground was near to constant at 8°. The emitted lidar sample point density, calculated from the acquisition parameters (**Table 1**), was greater than 3 per m^2, however the final point density can be significantly higher in areas of swath overlap and if emitted pulses record both first and last returns. All lidar and ground-truth data were georegistered to Universal Transverse Mercator (UTM) coordinates using two global positioning system (GPS) base stations located within the area that was surveyed (**Figure 2**).

Ground and vegetation surveys

Several differential kinematic GPS surveys were conducted over the study area from 27 to 30 August 2002 to locate reference points (RPs) for comparison with the lidar data. These surveys were conducted to establish RPs on ground surfaces that were (*i*) flat and level highway surfaces, to assess

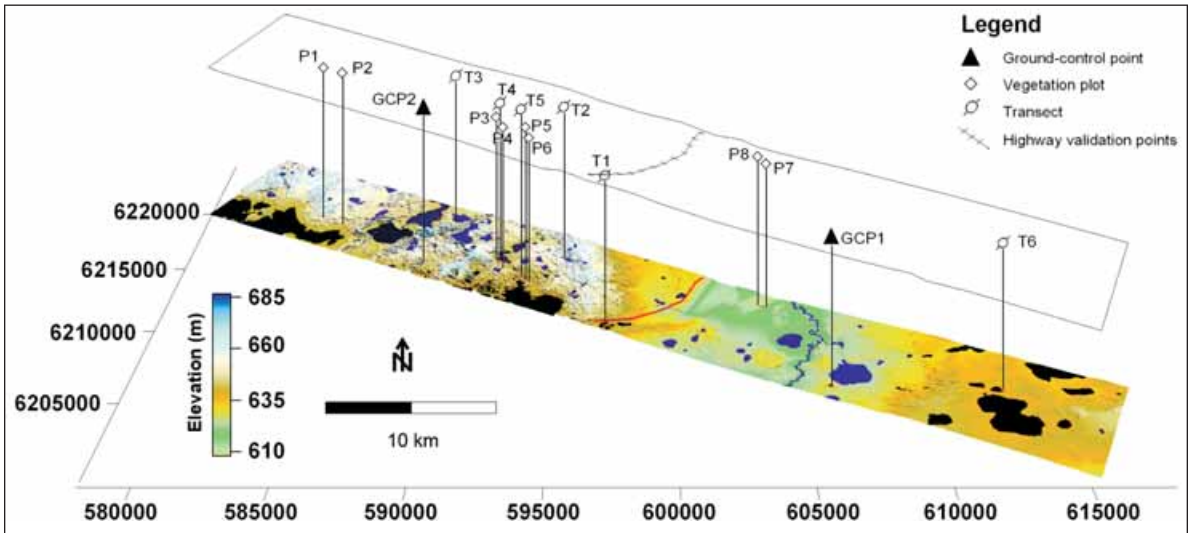

Figure 2. Utikuma survey polygon. Colour-coded ground DEM illustrating the locations of GPS base station ground-control points (GCP), highway reference point transects (crosses), forest plots (P1–P8), and vegetation transects (T1–T6). Open water corresponds to black areas in the DEM.

Table 1. Utikuma lidar survey Optech ALTM 2050 sensor, flight, and data collection configuration.

Sensor and flight settings	
Pulse rate	50 kHz
Scan frequency	36 Hz
Maximum scan angle	±16°
Aircraft velocity	<65 m/s
Flying altitude	<1200 m agl
Maximum bank angle	20°
Line spacing	300 m
No. of flight lines	20
Swath sidelap	>50%
Lidar data configuration	
Across-track spacing	~0.9 m
Along-track spacing	~1.0 m
Pulse foot print diameter	~0.3 m
Pulse positional error	<0.6 m
Ground swath width	>650 m
Ground coverage	>200%

Note: Pulse positional error was quoted by the manufacturer and was not directly assessed in this study.

the vertical accuracy of the raw lidar data; and (*ii*) covered by a short (<5 m tall) vegetated canopy, to compare with lidar data that had penetrated through the vegetation and had been classified as ground returns. These data were collected to quantitatively assess whether the lidar data were within expected tolerances, i.e., ±0.15 m (1 SD) for elevation data over well-defined surfaces. For less well defined vegetation-covered surfaces, the only known comparable statistics detailing vertical bias in ground elevation for a northern wetland environment range from +0.07 m (±0.15 m) to +0.15 m (±0.26 m) for graminoid and willow scrub, respectively (Töyrä et al., 2003). Analysis carried out by Hodgson and Bresnahan (2004) in South Carolina demonstrated both positive and negative absolute errors, from –0.06 m (±0.23 m) to +0.06 m (±0.19 m), in lidar ground elevation for various ground covers. These errors were largely attributed to lidar elevation and horizontal displacement error (Hodgson and Bresnahan, 2004).

Nonvegetated RPs were surveyed along road-centre and shoulder markings at 100 m intervals along a highway running the entire width of the survey polygon. (RMS errors in the GPS RP locations were in the millimetre to centimetre range and negligible compared with manufacturer-quoted lidar errors, which were expected to be up to 0.6 m.) RPs lying beneath vegetation cover were collected along six relatively flat transects of 30–60 m in length across heterogeneous ground cover types (**Figure 2**). Each transect was marked with stakes and a 30 m tape, and RPs were collected at equal intervals (from 0.5 to 2.0 m depending on local vegetation height variability). Ground cover types varied along the transects and were divided into four short vegetation classes (**Figure 3**) based on the Ducks Unlimited Canada vegetation classification of the Utikuma wetland complex (Ducks Unlimited Canada, 2002): (*i*) aquatic vegetation, AQ; (*ii*) grass and herbs, GH; (*iii*) low shrubs, LS (<2 m), and (*iv*) tall shrubs, TS (2–5 m).

At each transect RP, three measurements of maximum vegetation canopy height within a 0.5 m radius around that point were made with a measuring staff and the average noted along with a description of the vegetation type. These measurements were collected for comparison with heights derived from the lidar data. RP and vegetation height data were collected simultaneously to ensure coregistration of the data. Collecting canopy height and GPS data was challenging under tall canopies, and so only short vegetation classes could be investigated along transects. For tree vegetation classes, forest mensuration data were collected for a series of sample plots to characterize canopy height for subsequent comparison with plot-level lidar data. Two predominant end-member forest species belonging to the Ducks Unlimited Canada classifications of "needle leaf conifer" and "deciduous" were chosen for this analysis (**Figure 3**): (*i*) needle leaf conifers (black spruce, *Picea mariana*), BS; and (*ii*) deciduous (aspen, *Populus tremuloides*), AS.

Eight 15 m × 15 m plots were located using distance and bearing measurements to nearby RPs. Four plots each of aspen and black spruce were set up to represent deciduous and conifer end-member species, respectively. Homogeneous forest plots representing a range of height classes were sampled. Tree height and live crown length were measured using a vertex sonic hypsometer (for crown apices that were not distinct, the average of at least three measurements was recorded, with an uncertainty of up to ±0.5 m in worst cases), diameter at breast height (DBH) was measured with a standard DBH tape measure, and crown diameter was measured along north–south and east–west crown axes using a survey tape measure. In the aspen plots, all trees with a DBH greater than 9 cm were recorded. Trees with DBH less than 9 cm did not constitute a significant element in the overall canopy. For the black spruce plots, all stems above 2 m in height were recorded, as even trees with a small DBH could make up significant canopy elements for this conifer species.

Data analysis

Lidar data processing and accuracy assessment

Airborne GPS trajectory, ground GPS base station, on-board inertial reference system, scan angle, airborne laser terrain mapper (ALTM) calibration, and raw laser range data were combined within the Optech Incorporated proprietary REALM software to generate UTM coordinates for every first and last laser pulse return collected over the study area. Over hard impenetrable surfaces the first and last returns for every emitted pulse are coincident. Over areas of forest canopy, where light can penetrate to the ground, the first returns are preferentially distributed throughout the upper canopy, with the last returns nearer the ground. The laser pulse time interval meters within the ALTM hardware used in this study were unable to distinguish between first and last returns less than 4.6 m apart.

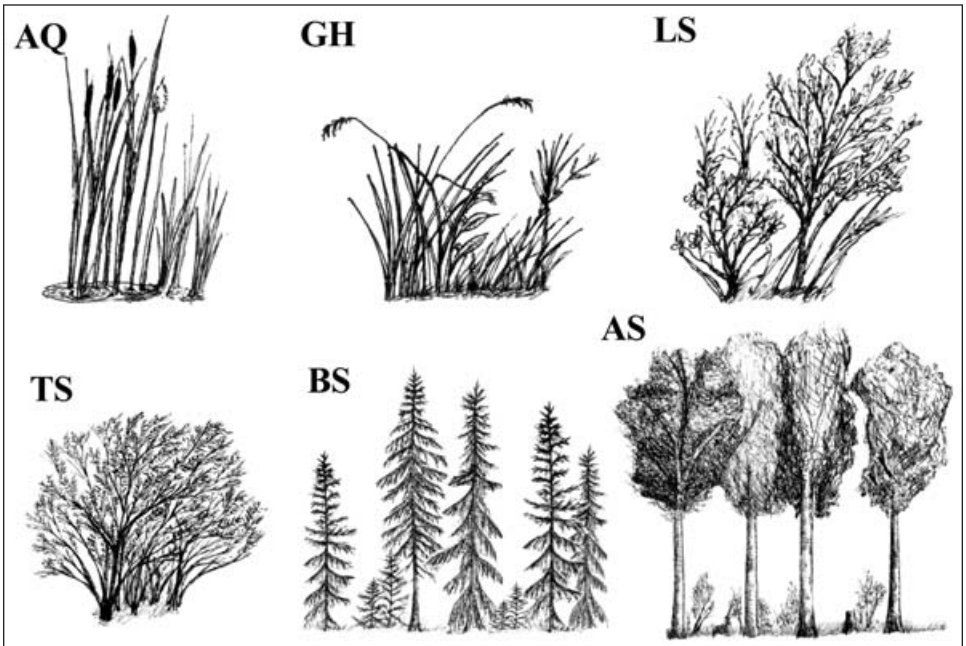

Figure 3. Vegetation classes sampled. Note that the individual diagrams are at different scales. AQ, aquatic vegetation; AS, aspen; BS, black spruce; GH, grass and herbs; LS, low shrubs (<2 m); TS, tall shrubs (2–5 m).

Therefore, only single (i.e., coincident first and last) returns can be recorded in canopies lower than this height. The raw lidar data were classified into ground and vegetation returns using an automated algorithm in proprietary software using filter parameters defined by the data collection service provider.

To assess the accuracy of the raw lidar elevation data, highway RPs were compared with lidar returns that were within a 0.5 m horizontal radius of an RP (error = lidar height minus RP height). The road was flat and all RPs were collected at least 1 m from the road edge. Therefore, the absolute vertical distance between an RP and the edge of a 0.5 m radius out from the centre was negligible. The highway traversed the entire width of the study area, and the RPs collected were compared with raw lidar data sampled from every flight line. Vegetated transect RPs were also compared with ground-classified lidar returns for the short vegetation classes to evaluate the influence of vegetation on lidar ground height accuracy. In areas of steep slope, positional error in the lidar data will introduce a vertical error component (e.g., Hodgson and Bresnahan, 2004). To remove the possibility of vertical errors due to positional uncertainty, highway and transect RPs were collected over areas of minimal relief.

Lidar rasterisation

Ground-classified lidar sample point densities are typically irregularly spaced over the ground surface owing to varying degrees of vegetation density. To determine lidar heights above ground level and to generate CHMs, the ground and vegetation data can be interpolated to a common raster array (e.g., Lim et al., 2003a). These two surfaces are referred to as DEM_{ground} and DEM_{canopy} for the bare-ground and vegetation canopy surfaces, respectively. In this study, both the ground surface and vegetation canopy height data were rasterised to a 1 m grid so that field-measured RPs and vegetation heights could be compared with their interpolated lidar equivalents.

All ground-classified data were rasterised to generate a 1 m resolution digital elevation model (DEM_{ground}). An inverse distance weighted routine was chosen because it maintains point integrity, enables interpolation using a simple distance weighted function, and is relatively fast (Golden Software Inc., 2002). A search radius of 10 m was chosen so that a surface would be interpolated in areas of sparse lidar data coverage. The highway and ground transect GPS control points were compared with the lidar DEM_{ground} to estimate absolute errors resulting from the interpolation.

The DEM_{canopy} for the survey polygon was rasterised from the vegetation-classified lidar data. To reduce the possibility of biasing the interpolated DEM_{canopy} model downwards, the lidar data were filtered so that only the highest laser pulse returns within each 0.5 m × 0.5 m window were used for rasterisation. As with the ground DEM, an inverse distance weighted rasterisation procedure was adopted, but the search radius was reduced to 1 m so that a vegetation canopy would not be interpolated in areas of no data. A raster CHM was then created by subtracting DEM_{ground} from DEM_{canopy}.

Lidar canopy surface height analysis

Short vegetation

To investigate laser pulse penetration into foliage, the lidar point-based estimates of canopy surface height for short vegetation were derived by extracting the highest laser pulse return from within a 0.5 m radius of every transect RP and

subtracting the RP elevation. The canopy lidar return was compared with the RP height rather than another lidar return at ground level, as the purpose of this analysis was to assess the level of vertical correspondence between the uppermost canopy lidar returns and the actual surface of the vegetation canopy. Raster-based estimates of canopy height were extracted from the CHM using the value of the 1 m × 1 m grid cell closest to each transect RP. The lidar point- and raster-based estimates of canopy surface height were then compared with field-measured heights. Summary statistics and regressions were performed for each short vegetation class to assess the error in lidar point- and raster-based estimates due to laser pulse foliage penetration. Some height error is to be expected owing to the inherent horizontal uncertainty (up to ~0.6 m) in the lidar x–y coordinate, and this error will be maximized in areas of variable canopy surface height.

Vegetation canopy volume (i.e., the volume between the canopy surface and the ground for each vegetation type across all transects) was calculated for the field and lidar point- and raster-based estimates to quantify the level of volume underestimation resulting from lidar height errors. For the sake of comparison, the planimetric area A_p of each field and lidar point- and raster-based estimate of vegetation height was taken to be 1 m × 1 m. A vertical frequency distribution of the number of measurements per height quantile q for each measurement type thus provided a measure of exposed canopy area at each quantile for each vegetation type across all the transects. Volume v was calculated by multiplying the quantile heights H_q by their respective frequencies F_q and summing the results:

$$v = \sum_{q=0}^{q=\max} (H_q F_q A_{p,r}) \quad (3)$$

Forest vegetation

To make a direct comparison of lidar point- and raster-based height estimates with the forest plot mensuration data, a half-ellipsoid tree crown model was employed to describe the vertical distribution of canopy surface exposure within each plot. The model used was similar to those described by Pollock (1996) and Nelson (1997) and has been used in other lidar canopy simulation studies (Holmgren et al., 2003). Tree height, crown length, and crown radius were the parameters necessary to model the plot-level canopy surface distribution. Although black spruce and aspens tend to have quite different shapes (**Figure 3**), the same half-ellipsoid function was applied to both because it was assumed that the major differences in crown shape would be accommodated by the measured differences in crown lengths and diameters. Other studies have also used the same function to describe a variety of tree types (e.g., Straub et al., 2001). By adopting an ellipsoidal model, as opposed to a spherical or conical model, potentially large errors are mitigated (Nelson, 1997).

A vertical frequency distribution of exposed canopy surface area was generated for each plot, and the average canopy surface height for each plot was calculated. Vertical area frequency distributions were also generated for both the first pulse return lidar and raster data for comparison (only first returns were considered, as these were assumed to most likely represent canopy surface). The lidar distribution was generated by first dividing the area of each plot into the total number of all laser pulse returns within the plot to calculate the area represented by each individual return A_r. The lidar data were then detrended to remove the influence of topography by subtracting the interpolated raster ground elevations associated with each lidar return, and a vertical frequency distribution of the number of returns multiplied by A_r was plotted at 1 m height quantile intervals. The raster CHM distribution was generated by plotting the vertical frequency of grid cells in each height quantile (A_r = 1 m^2 for each grid cell). Average canopy surface heights were considered to be the mean quantile height of the area frequency distributions. The volumes beneath the plot canopies using each method were calculated using Equation (3).

Results and discussion

Data output

The average dropout rate per flight line (lost laser pulse returns as a percentage of the total emitted pulses) was approximately 8%, with a maximum loss of 19% for flight lines over open water and a minimum loss of 1% for those over areas of dry land. The average point density for the entire polygon was between 2 and 5 points per square metre, depending on swath overlap, local dropout rate, and division of first and last returns. Following the automated vegetation classification, 24% of all the raw lidar data were classified as ground points. Therefore, the average point density of ground-classified returns over the survey polygon was between 0.5 and 1.3 returns per square metre. The ground class point density was highly variable, however, with higher densities over open dry ground and lower densities over areas of dense canopy and wet ground.

Lidar accuracy assessment

After subtracting highway RP elevations from laser pulse returns within a 0.5 m horizontal radius, the mean height difference was found to be 0.00 m with a standard deviation of 0.07 m. These results are consistent with those of Töyrä et al. (2003). The raster DEM comparison showed similar results (**Table 2**). These results demonstrate that the ALTM 2050 was correctly calibrated and performing within specification.

The average difference between ground-classified laser pulse returns and RPs collected from vegetated surfaces was +0.07 m (±0.16 m). Similar results were returned for the raster DEM and ground-control point comparison, with a mean offset of +0.04 m (±0.14 m) (**Table 2**). Laser pulse returns lying above RPs were also observed by Töyrä et al. (2003) in vegetated areas and can be explained by the reduced probability of laser pulse penetration to true ground level. It must also be noted that some error in ground return elevation is attributable to

Table 2. Ground-classified lidar and raster ground DEM height errors relative to GPS reference point heights for each land cover observed.

	Land cover					
	Highway	All ground data	Aquatic vegetation	Grass and herbs	Low shrubs	Tall shrubs
Raw lidar height error statistics						
Mean	0.00	+0.07	+0.15	+0.02	+0.06	+0.06
Min.	–0.18	–0.15	–0.15	–0.13	–0.09	+0.02
Max.	+0.25	+0.91	+0.91	+0.49	+0.49	+0.08
SD	0.07	0.16	0.22	0.10	0.12	0.03
N	95	127	35	45	43	4
P	nd	<0.01	<0.01	nd	<0.01	<0.01
Rasterised lidar height error statistics						
Mean	0.00	+0.04	+0.12	0.00	+0.01	+0.11
Min.	–0.19	–0.30	–0.10	–0.25	–0.30	–0.16
Max.	+0.13	+0.88	+0.88	+0.39	+0.31	+0.36
SD	0.08	0.14	0.18	0.10	0.13	0.16
N	95	208	45	77	72	14
P	nd	<0.01	<0.01	nd	nd	<0.01

Note: *N*, number of observations; nd, no significant height difference; *P*, tail probability of no difference in height.

misclassification of laser pulse returns by the classification algorithm used (Raber et al., 2002). For this study, however, the classification algorithm was kept spatially constant, and any variation in the magnitude of vertical error can be attributed to localized ground cover conditions. It is apparent that the vertical offset varied with vegetation type, with negligible offsets of +0.02 m (raw lidar) and 0.00 m (raster DEM) for the grass and herb class and relatively large offsets of +0.15 m (lidar) and +0.12 m (raster) for the aquatic vegetation class (**Table 2**).

Foliage orientation, height, and density and ground surface type can all potentially influence the likelihood of laser pulses reaching and reflecting from the true ground surface. The larger offset for aquatic vegetation is probably not a simple function of vegetation height, as both low shrub and tall shrub ground covers display taller vegetation heights (**Table 3**). Along the transects visited, aquatic vegetation was not noticeably denser than other vegetation types. Aquatic vegetation tended to have the most uniform structure, with most stems pointing upwards and a small planimetric surface area relative to other vegetation classes (**Figure 3**). With such a foliage arrangement, laser pulse penetration is somewhat dependent on incident scan angle (Davenport et al., 2000). For this study, however, the average scan angle incident on the ground was close to nadir at 8° and should therefore ensure a high rate of laser pulse penetration through the canopy. It is speculated that the relatively large average difference of 0.15 m between laser pulse return and RP height is related to the ground surface condition. The ground cover beneath most of the aquatic vegetation sampled tended to be open water or saturated organic soils. These types of ground cover reflect weakly in the 1064 nm infrared wavelength of the laser, and thus the likelihood of a ground return is reduced relative to drier and more reflective surfaces. In the absence of strong laser backscatter from the true ground surface, laser returns will therefore tend to be biased upwards into the more highly reflective foliage.

Vegetation canopy height and volume

Short vegetation

The six transects of field vegetation height measurements, filtered lidar heights above RPs, and raster CHM heights are illustrated in **Figure 4**, with comparative statistics presented by vegetation class in **Table 3**. There is some visual similarity between the field, point-based lidar, and raster CHM transects (**Figure 4**), suggesting that scanning lidar can approximately map vegetation canopy morphology, but there are some noticeable differences. **Figure 4** and **Table 3** demonstrate that there is a tendency for the filtered point-based laser returns (i.e., highest returns within a 0.5 m radius around the RP) to penetrate the vegetation canopy surface, but the amount of penetration is highly variable along the transects. (Although positional error in the lidar data will introduce some vertical error in canopy height estimation, the consistent underestimation of height (**Table 3**; **Figure 4**) indicates that positional uncertainty in the lidar returns is not the source of vertical bias.) In addition, the lidar and raster CHM transects frequently deviate from one another despite the CHM being interpolated from the lidar data. This is likely a function of ground height interpolation errors and the larger 1 m search radius used for raster interpolation compared with the 0.5 m search radius used to find the highest laser pulse relative to a GPS reference point.

Laser pulse penetration into foliage for each vegetation class is visually illustrated in the vertical area distribution plots in **Figure 5**. It is apparent from **Table 3** and **Figure 5** that the amount of foliage penetration, and therefore point-based lidar and raster CHM underestimation of vegetation height and volume, varied with vegetation type. Average foliage penetration ranged from 0.10 m (33%, $P < 0.05$) for the grass

Table 3. Field, lidar, and raster CHM vegetation height error statistics for short (<5 m) vegetation classes.

	Vegetation class			
	Aquatic vegetation	Grass and herbs	Low shrubs <2 m	Tall shrubs 2–5 m
Field height measures				
Avg.	0.45	0.30	0.82	3.76
Min.	0.01	0.05	0.10	2.30
Max.	1.00	0.80	2.00	5.00
SD	0.25	0.20	0.59	0.94
N[a]	27 (49)	31 (77)	44 (71)	12 (16)
Point-based lidar height statistics				
Avg.	0.21	0.20	0.30	2.92
Min.	–0.04	–0.02	–0.07	0.10
Max.	0.52	0.83	1.48	5.03
SD	0.14	0.20	0.31	1.46
N[a]	27 (40)	31 (57)	44 (55)	12 (12)
Rasterised lidar CHM statistics				
Avg.	0.16	0.26	0.43	2.67
Min.	0.03	–0.04	–0.01	1.19
Max.	0.55	0.91	1.76	4.70
SD	0.12	0.26	0.38	1.30
N[a]	27 (32)	31 (44)	44 (55)	12 (16)
Comparative statistics				
Point-based lidar vs. field				
Mean difference[b]	–0.24 (53%)	–0.10 (33%)	–0.52 (63%)	–0.84 (22%)
P	<0.01	<0.05	<0.01	<0.10
Rasterised lidar vs. field				
Mean difference[b]	–0.29 (64%)	–0.04 (13%)	–0.39 (48%)	–1.09 (29%)
P	<0.01	>0.10	<0.01	<0.05

Note: *P*, tail probability of no difference to field measured heights.
[a]Comparative sample used for generation of statistics. The values in parentheses are the total number of data collected.
[b]Lidar canopy height minus field canopy height.

and herb class to 0.84 m (22%, $P < 0.10$) for the tall shrub class. Low shrubs displayed the highest proportion of vegetation surface underestimation, however, with average laser pulse penetration of 63% (0.52 m, $P < 0.01$) into the vertical foliage profile. The relatively open structure of low shrubs (i.e., space between stems) compared to other classes (**Figure 3**) likely allows greater penetration of a laser pulse into the foliage before sufficient energy is backscattered to register a signal within the electro-optical sensors of the ALTM. Aquatic vegetation also demonstrates a high proportion of foliage laser pulse penetration (53%, $P < 0.01$), and this is likely due to its generally vertical foliage orientation projecting a minimal planimetric surface area exposure (**Figure 3**). The average aquatic vegetation raster CHM estimate displays the greatest difference from field measurements (64%, $P < 0.01$), and this is likely a function of both (*i*) increased laser penetration into foliage, and (*ii*) overestimation of true ground surface height beneath this kind of vegetation (**Table 2**).

The relationships between measured vegetation canopy heights and the corresponding lidar-derived estimates for transect measurements are illustrated in **Figure 6** (data below 2 m vegetation height have been resampled to keep every third point to create a more uniform distribution for regression analysis). After performing linear regression on each individual vegetation class (**Table 4**), it is apparent that there is a statistically significant relationship between the point-based lidar and field vegetation height measures for all classes. The relationship between field and raster CHM measures are weaker in all cases, and the relationship is not significant at the 99% confidence level for aquatic and low shrub classes. All coefficient of determination values returned for regression lines passing through the origin (0 m vegetation height) for all but the tall shrub vegetation classes were null and indicate that the true vegetation heights cannot be predicted using a simple multiplication factor of the lidar or raster CHM estimates. Intuitively, even the regression results demonstrating a weak but significant relationship are not appropriate because in each case the offset value *C* would result in a systematic overestimate of the minimum vegetation height. This is problematic for the three shortest vegetation classes (<2 m) because at least 20% of the field measurements made in each

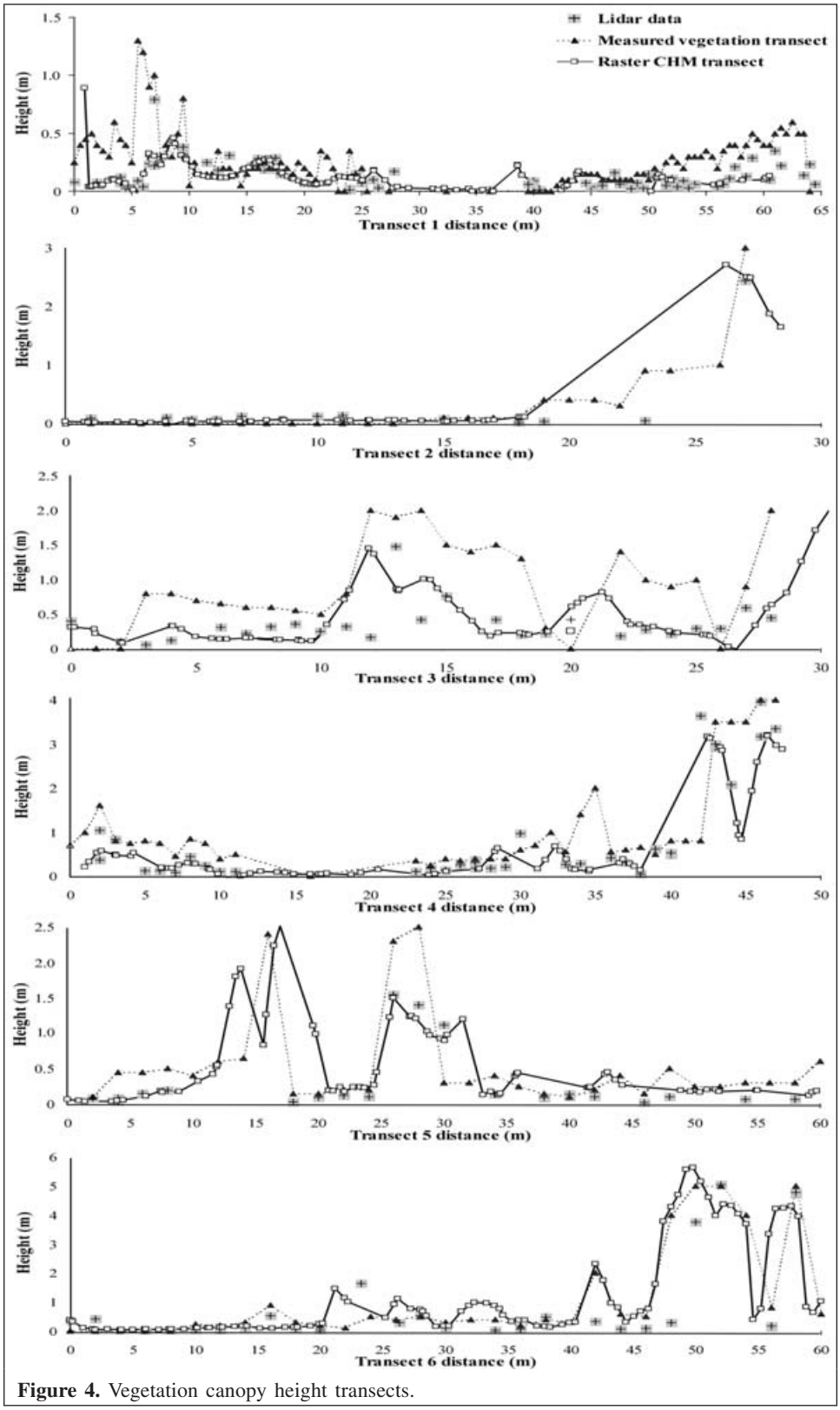

Figure 4. Vegetation canopy height transects.

class fall below the minimum heights determined from the regression analyses.

In addition to the minimum height problem, a further difficulty with the adoption of simple multiplication and offset regression models to correct lidar and raster height measures is that the slope gradients are below 1:1 and tend to underestimate the natural variance canopy surface height. This might be acceptable if the lidar and raster estimates displayed greater

variability than the field measures, but it is apparent from **Table 3** that the field-measured height data actually have similar or even greater standard deviations. Therefore, although the adoption of such models could lead to better estimates of average height within a class, they would systematically ignore the lowest vegetation while smoothing out the natural heterogeneity in canopy surface morphology. Smoothing out vegetation canopy morphology is problematic if lidar-derived canopy height data are used to map hydraulic roughness coefficients over the land surface.

Forest vegetation

Figure 7 demonstrates that modeled average canopy surface height derived from mensuration data is a good predictor of both plot-level average and Lorey height for end-member forest species of aspen and black spruce. It can be assumed, therefore, that such canopy surface model height estimates are reasonable predictors of plot-level tree heights for a variety of species within the study area. From the regression analysis presented in **Figure 7**, it is apparent that the canopy surface model estimate of average tree height tends to underestimate Lorey height for

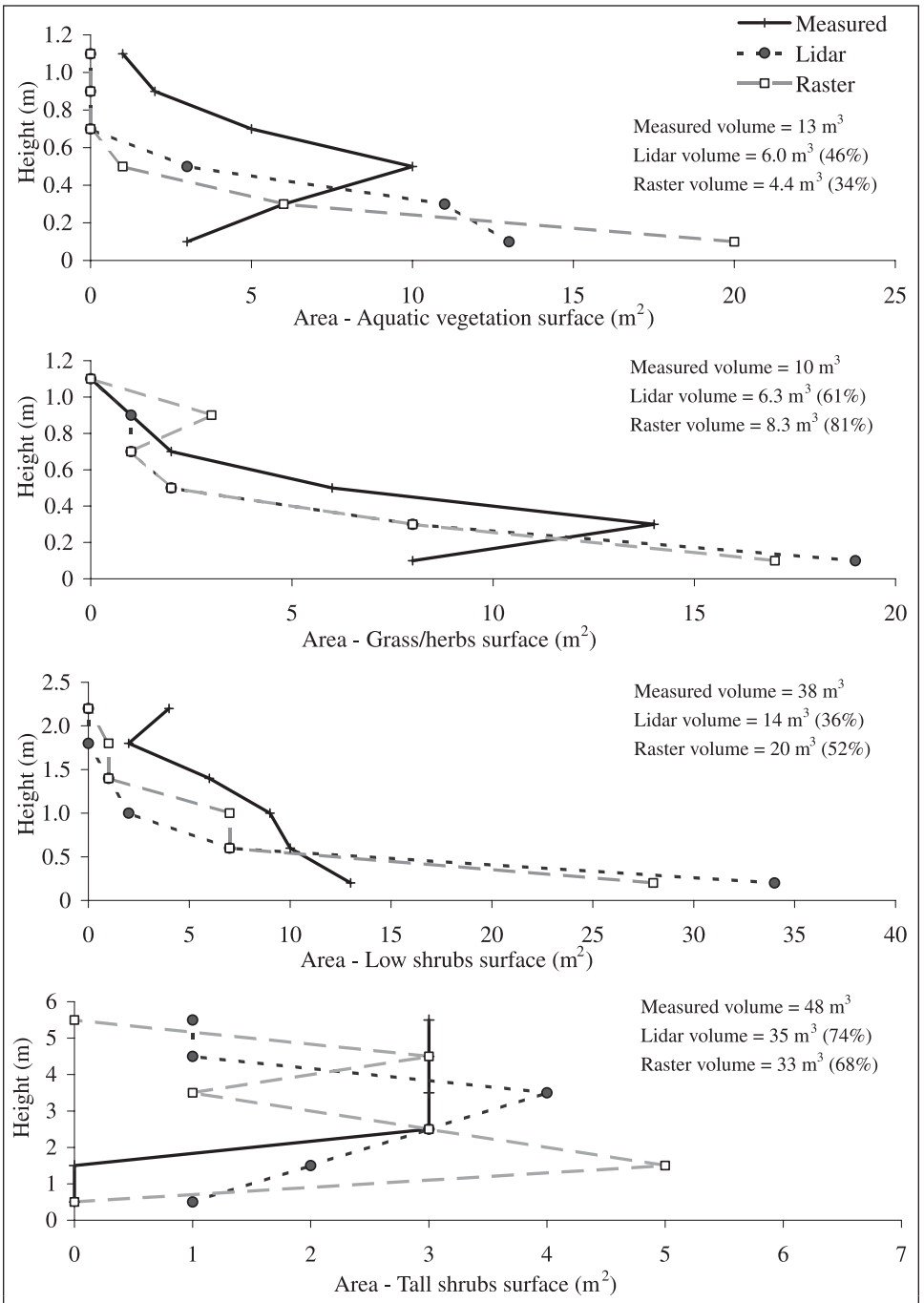

Figure 5. Vegetation area distributions per height quantile for each short vegetation class. Volume beneath upper vegetation surface estimates are inset.

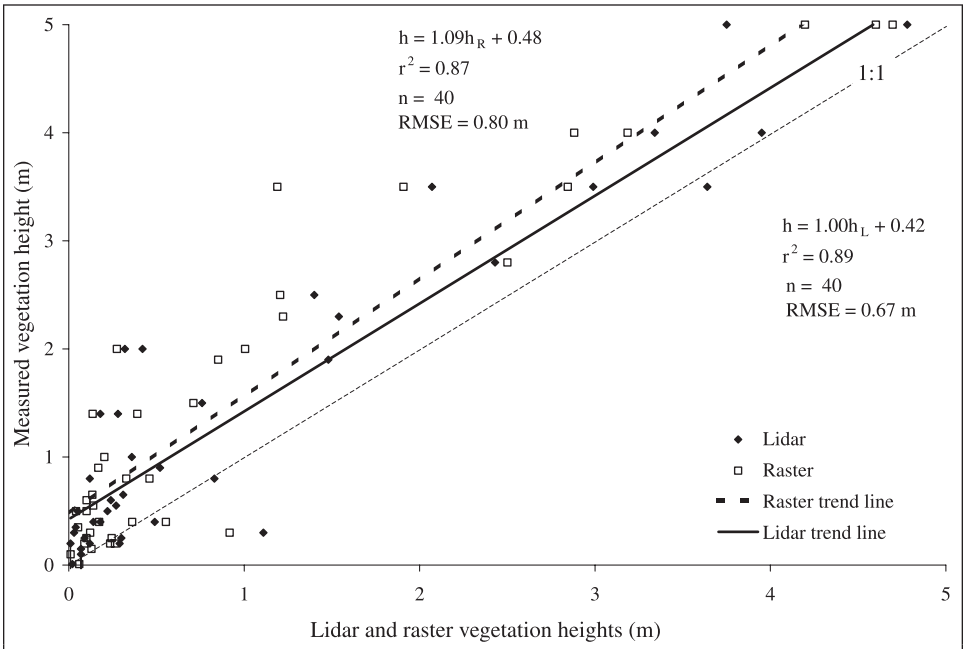

Figure 6. Plot of short vegetation height data versus lidar and raster height data per transect and vegetation class. Plotted data were thinned below 1 m measured vegetation height to even out distribution of points along the axes for regression analysis. *h*, vegetation height; L, point-based lidar; R, raster CHM; RMSE, root mean square error.

Table 4. Linear regression statistics for plots of vegetation height versus corresponding point-based lidar (L) and interpolated raster lidar CHM (R) height measurements.

	Aquatic vegetation (N = 27)		Grass and herbs (N = 31)		Low shrubs (N = 44)		Tall shrubs (N = 12)		All classes (N = 40)	
Statistic	L	R	L	R	L	R	L	R	L	R
$h = Ah_{L,R} + C$										
r^2	0.29	0.04	0.38	0.09	0.19	0.11	0.82	0.81	0.89	0.87
A	0.91	0.40	0.62	0.23	0.79	0.60	0.73	0.67	1.00	1.09
C	0.26	0.39	0.18	0.24	0.49	0.62	1.43	1.89	0.42	0.48
P	<0.01	0.32	<0.01	0.10	<0.01	0.03	<0.01	<0.01	<0.01	<0.01
$h = Ah_{L,R}$										
r^2	0	0	0	0	0	0	0.54	0.11	0.84	0.80
A	1.80	1.90	1.10	0.71	1.80	1.30	1.10	1.20	1.14	1.26

Note: The results for All classes data are presented in **Figure 6**. *P* values <0.01 denote that the correlation is significant at the 99% confidence level. *A*, gradient; *C*, offset; *h*, vegetation height; L, point-based lidar; R, interpolated raster lidar CHM.

the eight plots studied, with a mean difference of >1 m. The mean difference between plot-level average tree height and modeled canopy surface height is <0.2 m, and the regression line is close to the 1:1 slope.

Average plot-level canopy surface heights derived from vertical lidar and raster CHM area distributions compare favourably with heights derived from forest mensuration modeled area distributions, with coefficient of determination values of 0.99 (point-based lidar) and 0.96 (raster CHM) (**Figure 8**). The relationships in both cases are close to unity, with small multiplication factors of 1.06 (lidar) and 1.10 (raster CHM). The data presented in **Figures 7** and **8** indicate that the lidar- and raster-generated vertical canopy surface area distributions would be good predictors of plot-level average tree and canopy surface heights. This is demonstrated in the coefficients of determination for lidar (r^2 = 0.96, slope = 1.12) and raster (r^2 = 0.97, slope = 1.07) canopy surface height predictions of plot-level average tree height (not shown).

The slightly greater than unity slope gradients in **Figure 8** suggest either that laser pulses penetrate slightly into the foliage or that the tops of the tallest trees are not adequately sampled. This is better illustrated in the combined vertical canopy surface area distributions for all of the aspen and black spruce plots in **Figure 9**. This general finding is in agreement

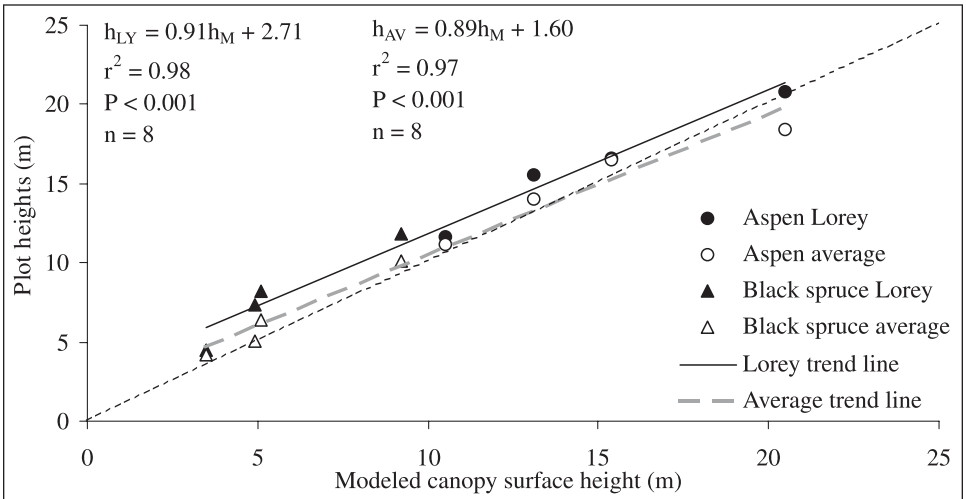

Figure 7. Plot-level average tree and Lorey heights versus modeled canopy surface heights for both deciduous aspen and conifer black spruce forest plots. h_{AV}, plot average tree height; h_{LY}, Lorey height; h_M, average height of modeled canopy surface.

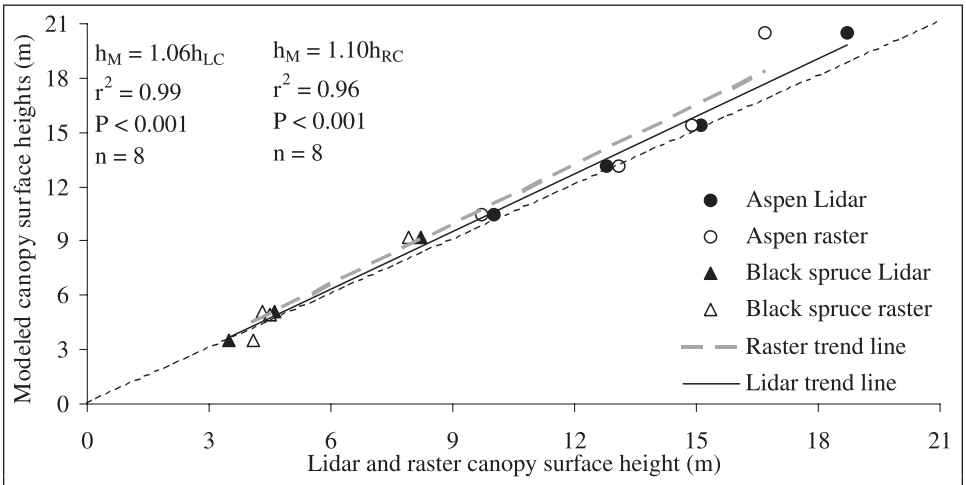

Figure 8. Plot-level modeled canopy surface heights versus lidar and raster canopy surface heights for aspen and black spruce plots. h_{LC}, average height of lidar canopy surface; h_M, average height of modeled canopy surface; h_{RC}, average height of raster CHM.

with findings from other studies (Magnussen et al., 1999; Gaveau and Hill, 2003). Although both forest end-member types display a similar underestimation of exposed vegetation area at the upper height quantiles, the two distributions differ markedly at the lower height quantiles. For the aspen species with well-defined canopy top and base, there appears reasonable correspondence between the mensuration data modeled, point-based lidar and raster CHM canopy surface area distributions in the lower canopy. Overall, the underestimation of upper canopy area combined with a reasonable estimate of lower canopy area leads to an approximately 10% underestimate in the total canopy volume for aspen trees (**Figure 9**). However, the canopy surface area at the mid to lower height quantiles (above undergrowth layer) in the black spruce plots is overestimated in the lidar and raster distributions. This leads to overestimates of black spruce canopy volume of 3% (point-based lidar) and 26% (raster CHM) despite underestimating the canopy surface area at the upper quantiles.

Given that significant foliage penetration was observed in the short vegetation classes (**Table 3**; **Figure 5**) and that Gaveau and Hill (2003) observed this phenomena directly for trees, it can be assumed that laser penetration into the canopy is partly responsible for the underestimation of exposed canopy surface area in the upper height quantiles (**Figure 9**). It should be noted, however, that the two forest end-member classes differ markedly in canopy morphology, with relatively large crowns and closed canopy for the aspens and small crowns with open canopy for the black spruce. The smaller conifer tree crowns result in a reduced likelihood of a laser pulse sampling the upper quantiles of an individual tree and therefore systematically bias the sample distribution downwards. This is

evidenced in the canopy surface area distributions in **Figure 9**, where this bias has led to an apparent downshift in the overall black spruce distribution and an overestimation of area at the lower quantiles. These data, therefore, demonstrate influences of both laser pulse foliage penetration and laser pulse sample density.

Hydraulic roughness sensitivity analysis

If lidar-derived raster CHM estimates are used in hydrometeorological models to directly estimate ground cover frictional properties, then predicted aerodynamic and hydraulic resistance coefficients will be sensitive to lidar height errors. Using the same Darcy–Weisbach friction factor calculations as those presented by Mason et al. (2003), class-dependent shear velocity and elasticity parameter values from Kouwen (1988) and Kouwen and Fathi-Maghadam (2000), a constant slope of 0.001 (from Utikuma DEM), a water depth of 1 m, and a subcritical shear velocity of 0.1 m/s, it was possible to estimate a set of hypothetical friction factors for each vegetation class (**Table 5**). Elasticity values for tall and intermediate vegetation were all treated like spruce vegetation (Kouwen, 1988).

Friction factor values were underestimated by up to 54% for vegetation classes shorter than 2 m but overestimated by up to 41% for tall and intermediate height vegetation classes (**Table 5**). In the example given here, f increased for tall and intermediate height classes because of an increase in the ratio of water depth to vegetation height (short vegetation is effectively submerged) and implicit assumptions about the vegetation class shape, density, rigidity, and flexibility. This could potentially occur in cases where field data are collected to establish the structural properties of individual classes of vegetation, and then lidar data are used to create high-resolution (i.e., grid cell resolution approaching raw lidar point spacing) raster vegetation height maps.

Conclusions

This study has provided an assessment of lidar-based errors in ground elevation and vegetation height and a sensitivity analysis of hydrological friction parameter estimates for six dominant vegetation classes within a boreal wetland environment. Comparing raw lidar data points with 95 highway reference points collected across the entire survey polygon revealed no vertical bias. The standard deviation in the lidar data over the RPs was ±0.07 m. After subtracting field GPS elevations from ground-classified lidar data for 127 RPs over vegetated transects, an average bias of +0.07 (±0.16 m) was found (+0.04 m in rasterised lidar data). The observation of ground height errors in vegetated areas is consistent with the findings of other studies (Töyrä et al., 2003; Hodgson and Bresnahan, 2004). The vertical bias was found to vary with vegetation cover, from no significant difference for grass and herbs to +0.15 m for aquatic vegetation. It is believed that lidar ground height estimation was most problematic for aquatic vegetation owing to weak laser backscatter from the saturated ground conditions typically associated with this vegetation class. These observations support the rationale that ground

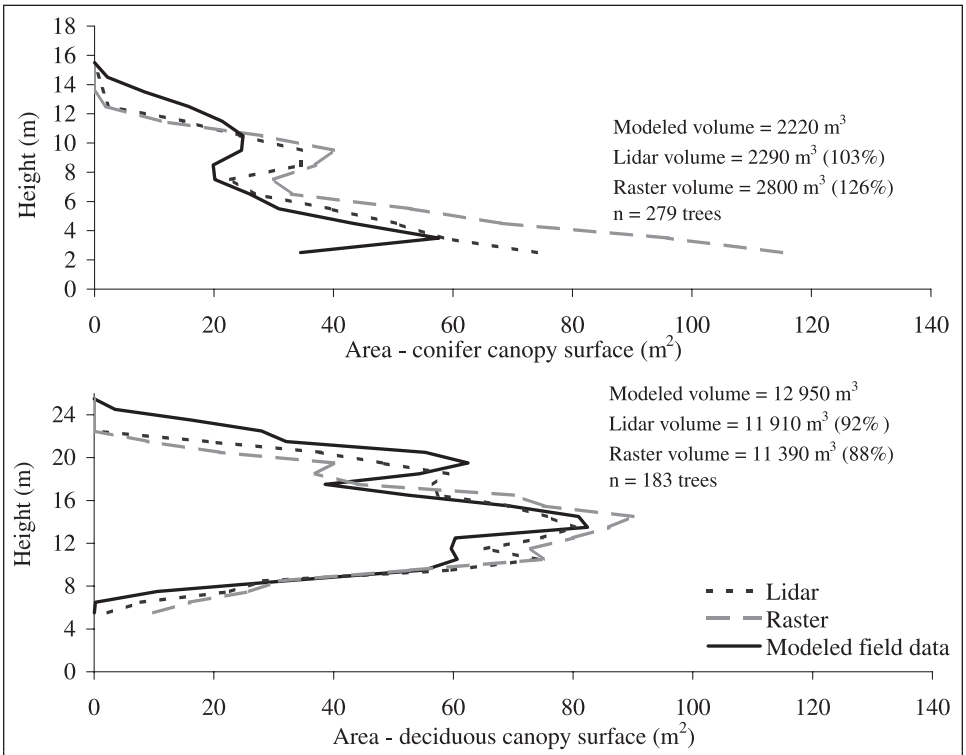

Figure 9. Combined canopy surface area distributions per height quantile for all plots within each forest vegetation class. Canopy volume estimates are inset.

Table 5. Friction parameters calculated from field and raster lidar CHM measurements for each vegetation class.

Vegetation class	Field	Raster CHM
Short vegetation (<2 m)		
Grass and herbs	0.46	0.41 (–10%)
Aquatic	0.64	0.30 (–54%)
Low shrubs	1.22	0.62 (–49%)
Tall and intermediate vegetation (>2 m)		
Tall shrubs	0.84	1.18 (41%)
Black spruce	0.47	0.55 (18%)
Aspen	0.21	0.23 (12%)

level lidar point classification should be vegetation class dependent (e.g., Cobby et al., 2001).

After filtering the data for local maxima, the penetration of vegetation-classified first-pulse lidar returns into the canopy surface was found to vary with vegetation class and range from 0.10 to 0.84 m. Maximum proportional foliage penetration was found to occur in low shrub vegetation (>60%), and this was thought owing to the relatively open structure and low foliage density typical of this vegetation class. Aquatic vegetation was also susceptible to a high proportion (>50%) of laser pulse foliage penetration, and this was thought related to the generally uniform and vertical orientation (minimal planimetric area projection) of aquatic vegetation in the study area. The tendency for both poor ground and canopy surface definition from lidar data in the aquatic vegetation class results in the greatest underestimations of height and canopy volume and the largest errors in friction factor (–54%) parameter estimation. This is an important observation because aquatic vegetation is associated with open water, and therefore estimates of hydrological friction parameters are more critical in this class than in any of the others.

Despite a systematic underestimation of height for all vegetation classes, it was found that lidar canopy surface heights were significantly correlated with measured heights at the 99% confidence level (r^2 from 0.19 to 0.82). Raster CHM measures were less significantly correlated with field measures, with all but aquatic vegetation being significant at the 90% confidence level (r^2 from 0.04 to 0.84). Linear regression models relating lidar and field height measures were considered of little practical value, however, because of the systematic smoothing of vegetation height variance and overestimation of minimum heights that would occur if they were adopted.

Actual forest canopy surfaces could not be compared directly with canopy laser pulse returns, but after modeling canopy surface area distributions from forest mensuration data, a quantile-to-quantile comparison could be made with similar distributions generated from the frequency of all lidar returns and CHM grid cells. It was found that the average canopy surface heights derived from the lidar point-based area frequency distributions were good predictors of average plot-level tree height (r^2 = 0.97). Height and volume were both underestimated by 3% and 8%, respectively, for the aspen plots, presumably influenced by laser pulse foliage penetration. For the black spruce plots, it was found that, although lidar height was underestimated by 10%, the canopy surface volume was actually overestimated by 3% and 26% for the lidar point-based and raster CHM distributions, respectively. The increased volume estimate is a function of the lidar and raster CHM model of vertical canopy surface area distribution overrepresenting the intermediate and low foliage heights in the plots.

It was found that underestimation of vegetation height from canopy lidar returns can introduce errors in land surface friction parameters that potentially exceed 50% for short (<2 m) vegetation and 40% for tall shrub vegetation and approach 20% for forest vegetation. Caution must, therefore, be exercised when directly estimating vegetation heights from canopy lidar returns if these estimates are to be used as the basis for the calculation of hydrological model parameters. Either vegetation class dependent corrections should be established and applied to direct lidar height measures, or low-resolution height estimates can be modeled from the spatial variance in the lidar data (Davenport et al., 2000). Although this paper has quantified vegetation class dependent foliage penetration and ground and canopy surface height biases, more research is needed into robust lidar height correction techniques that can be applied to both tall and short vegetation belonging to a variety of species classes.

Acknowledgements

The authors acknowledge the Canadian Consortium for LiDAR Environmental Applications Research for coordinating both ground and airborne data collection logistics; Optech Incorporated, notably Mr. Jim Green, for access to the ALTM 2050; John Barlow, Ron Chasmer, Rodney Clark, and Stella Heenan for assistance in the field; and Airborne Energy Solutions for providing an aircraft and flight crew for the lidar survey. Dr. Hopkinson gratefully acknowledges partial postdoctoral funding through a grant awarded to Dr. Treitz by the Centre for Research in Earth and Space Technologies, an Ontario Centre of Excellence. Dr. Creed and Dr. Treitz would also like to acknowledge financial support through the Natural Sciences and Engineering Research Council of Canada (NSERC) Collaboration Research and Development Grant, with partners from Alpac Ltd., Weyerhauesuer Ltd., and Ducks Unlimited Canada to Creed and NSERC Discovery Grant to Treitz.

References

Baltsavias, E.P. 1999. Airborne laser scanning: basic relations and formulas. *ISPRS Journal of Photogrammetry and Remote Sensing*, Vol. 54, pp. 199–214.

Bowen, Z.H., and Waltermire, R.G. 2002. Evaluation of light detection and ranging (LIDAR) for measuring river corridor topography. *Journal of the American Water Resources Association*, Vol. 38, pp. 33–41.

Cobby, D.M., Mason, D.C., and Davenport, I.J. 2001. Image processing of airborne scanning laser altimetry data for improved river flood modelling. *ISPRS Journal of Photogrammetry and Remote Sensing*, Vol. 56, pp. 121–138.

Cobby, D.M., Mason, D.C., Horritt, M.S., and Bates, P.D. 2003. Two-dimensional hydraulic flood modelling using a finite-element mesh decomposed according to vegetation and topographic features derived from airborne scanning laser altimetry. *Hydrological Processes*, Vol. 17, pp. 1979–2000.

Crawford, T.M., and Bluestein, H.B. 2000. An operational, diagnostic surface energy budget model. *Journal of Meteorology*, Vol. 39, pp. 1196–1217.

Davenport, I.J., Bradbury, R.B., Anderson, G.Q.A., Hayman, G.R.F., Krebs, J.R., Mason, D.C., Wilson, J.D., and Veck, N.J. 2000. Improving bird population models using airborne remote sensing. *International Journal of Remote Sensing*, Vol. 21, pp. 2705–2717.

Devito, K.J., Bayley, S.E., Creed, I.F., and Foote, A.L. 2000. *Hydrology, ecology, and disturbance of western boreal wetlands*. Natural Sciences and Engineering Research Council of Canada (NSERC), Ottawa, Collaboration Research and Development (CRD) Proposal.

Ducks Unlimited Canada. 2002. *Utikuma Lake, Alberta earth cover classification user's guide*. Ducks Unlimited Canada, Edmonton, Alta., and Ducks Unlimited, Inc., Rancho Cordova, Calif. 63 pp.

Fathi-Maghadam, M., and Kouwen, N. 1997. Nonrigid, nonsubmerged, vegetative roughness on floodplains. *Journal of Hydraulic Engineering, ASCE*, Vol. 123, No. 1, pp. 51–57.

Gaveau, D., and Hill, R.A. 2003. Quantifying canopy height underestimation by laser pulse penetration in small footprint airborne laser scanning data. *Canadian Journal of Remote Sensing*, Vol. 29, No. 5, pp. 650–657.

Golden Software Inc. 2002. *Surfer® for Windows, version 8: user's guide.* Golden Software Inc., Golden, Colo.

Gutelius, W. 1998. Engineering applications of airborne scanning lasers: reports from the field. *Photogrammetric Engineering & Remote Sensing*, Vol. 64, pp. 246–253.

Heinzer, T., Sebhat, M., Feinberg, B., and Kerper, D. 2000. The use of GIS to manage LIDAR elevation data and facilitate integration with the MIKE21 2-D hydraulic model in a flood inundation decision support system. In *Proceedings of the 20th Annual ESRI User Conference*, 26–30 June 2000, San Diego, Calif. Environmental Systems Research Institute (ESRI), Redlands, Calif. Available from http://gis.esri.com/library/userconf/proc00/professional/papers/PAP675/p675.htm [accessed 21 April 2005].

Hodgson, M.E., and Bresnahan, P. 2004. Accuracy of airborne lidar-derived elevation: empirical assessment and error budget. *Photogrammetric Engineering & Remote sensing*, Vol. 70, pp. 331–340.

Holmgren, J., Nilsson, M., and Olsson, H. 2003. Simulating the effects of lidar scanning angle for estimation of mean tree height and canopy closure. *Canadian Journal of Remote Sensing*, Vol. 29, No. 5, pp. 623–632.

Kouwen, N. 1988. Field estimation of the biomechanical properties of grass. *Journal of Hydraulics Engineering, ASCE*, Vol. 26, pp. 559–568.

Kouwen, N., and Fathi-Maghadam, M. 2000. *Journal of Hydraulics Engineering, ASCE*, Vol. 126, pp. 732–740.

Lim, K., Treitz, P., Baldwin, K., Morrison, I., and Green, J. 2003a. Lidar remote sensing of biophysical properties of tolerant northern hardwood forests. *Canadian Journal of Remote Sensing*, Vol. 29, No. 5, pp. 658–678.

Lim, K., Treitz, P., Wulder, M., St-Onge, B., and Flood, M. 2003b. LiDAR remote sensing of forest structure. *Progress in Physical Geography*, Vol. 27, pp. 88–106.

Maclean, G.A., and Krabill, W.B. 1986. Gross-merchantable timber volume estimation using an airborne lidar system. *Canadian Journal of Remote Sensing*, Vol. 12, No. 1, pp. 7–18.

Magnussen, S., and Boudewyn, P. 1998. Derivations of stand heights from airborne laser scanner data with canopy-based quantile estimators. *Canadian Journal of Forest Research*, Vol. 28, pp. 1016–1031.

Magnussen, S., Eggermont, P., and LaRiccia, V.N. 1999. Recovering tree heights from airborne laser scanner data. *Forest Science*, Vol. 45, pp. 407–422.

Mason, D.C., Cobby, D.M., Horritt, M.S., and Bates, P.D. 2003. Floodplain friction parameterization in two-dimensional river flood models using vegetation heights derived from airborne scanning laser altimetry. *Hydrological Processes*, Vol. 17, pp. 1711–1732

Means, J.E., Acker, S.A., Fitt, B.J., Renslow, M., Emerson, L., and Hendrix, C.J. 2000. Predicting forest stand characteristics with airborne scanning Lidar. *Photogrammetric Engineering & Remote Sensing*, Vol. 66, pp. 1367–1371.

Menenti, M., and Ritchie, J.C. 1994. Estimation of effective aerodynamic roughness of Walnut Gulch watershed with laser altimeter measurements. *Water Resources Research*, Vol. 30, pp. 1329–1337.

Næsset, E. 1997. Determination of mean tree height of forest stands using airborne laser scanner data. *ISPRS Journal of Photogrammetry and Remote Sensing*, Vol. 52, pp. 49–56.

Næsset, E. 2002. Predicting forest stand characteristics with airborne scanning laser using a practical two-stage procedure and field data. *Remote Sensing of Environment*, Vol. 80, pp. 88–99.

Næsset, E., and Økland, T. 2002. Estimating tree height and tree crown properties using airborne scanning laser in a boreal nature reserve. *Remote Sensing of Environment*, Vol. 79, pp. 105–115.

National ecological framework for Canada. 1996. *A national ecological framework for Canada*. Ecological Stratification Working Group, Research Branch, Agriculture and Agri-Food Canada, Ottawa, Ont. 125 pp.

Nelson, R. 1997. Modeling forest canopy heights: the effects of canopy shape. *Remote Sensing of Environment*, Vol. 60, pp. 327–334.

Pollock, R. 1996. *The automatic recognition of individual trees in aerial images of forests based on a synthetic tree crown image model*. Ph.D. thesis, University of British Columbia, Vancouver, B.C.

Popescu, S.C., Wynne, R.H., and Nelson, R.F. 2002. Estimating plot-level tree heights with lidar: local filtering with a canopy-height based variable window size. *Computers and Electronics in Agriculture*, Vol. 37, pp. 71–95.

Raber, G.T., Jensen, J.R., Schill, S.R., and Schuckman, K. 2002. Creation of digital terrain models using an adaptive lidar vegetation point removal process. *Photogrammetric Engineering & Remote Sensing*, Vol. 68, pp. 1307–1315.

Reutebuch, S.E., McGaughey, R.J., Andersen, H.-E., and Carson, W.W. 2003. Accuracy of a high-resolution lidar terrain model under a conifer forest canopy. *Canadian Journal of Remote Sensing*, Vol. 29, No. 5, pp. 527–535.

Ritchie, J.C. 1995. Airborne laser altimeter measurements of landscape topography. *Remote Sensing of Environment*, Vol. 53, pp. 91–96.

Rowe, J.S. 1972. *Forest regions of Canada*. Canadian Forestry Service, Department of the Environment, Ottawa, Ont., Publication 1300.

Schaudt, K.J., and Dickinson, R.E. 2000. An approach to deriving roughness length and zero-plane displacement height from satellite data, prototyped with BOREAS data. *Agricultural and Forest Meteorology*, Vol. 104, pp. 143–155.

Schindler, D.W. 1997. Widespread effects of climatic warming on freshwater ecosystems in North America. *Hydrological Processes*, Vol. 11, pp. 1043–1067.

Schindler, D.W. 1998. A dim future for boreal water and landscapes. *BioScience*, Vol. 48, pp. 157–164.

Smith, W., and Lee, P. (Editors). 2000. *Canada's forests at a crossroads: an assessment in the year 2000*. World Resources Institute, Washington, D.C. 107 pp.

St-Onge, B., Treitz, P., and Wulder, M. 2003. Tree and canopy height estimation with scanning lidar. In *Remote sensing of forest environments: concepts and case studies*. Edited by S. Franklin and M. Wulder. Kluwer Academic Publishers, Dordrecht, The Netherlands. pp. 489–509.

Straub, B.M., Gerke, M., and Koch, A. 2001. Automatic extraction of trees and buildings from image and height data in an urban environment. In *Proceedings of the International Workshop on Geo-Spatial Knowledge Processing for Natural Resource Management*, 28–29 June 2001, University of Insubria, Varese, Italy. Edited by A. Belward, E. Binaghi, P.A. Brivio, G.A. Lanzarone, and G. Tosi. pp. 59–64.

Töyrä, J., Pietroniro, A., Hopkinson, C., and Kalbfleisch, W. 2003. Assessment of airborne scanning laser altimetry (lidar) in a deltaic wetland environment. *Canadian Journal of Remote Sensing*, Vol. 29, No. 6, pp. 718–728.

Weltz, M.A., Ritchie, J.C., and Fox, H.D. 1994. Comparison of laser and field measurements of vegetation height and canopy cover. *Water Resources Research*, Vol. 30, pp. 1311–1319.

Winter, T.C., and Rosenberry, D.O. 1998. Hydrology of prairie pothole wetlands during drought and deluge: a 17-year study of the Cottonwood Lake wetland complex in North Dakota in the perspective of longer term measured and proxy hydrological records. *Climatic Change*, Vol. 40, pp. 189–209.

Witte, C., Dowling, R., Weller, D., Denham, R., and Rowland, T. 2001. Quantifying riparian vegetation and stream bank form through the use of airborne laser scanning and digital video data. In *IGARSS'01, Proceedings of the IEEE International Geoscience and Remote Sensing Symposium*, 9–13 July 2001, Sydney, Australia. Edited by T.I. Stein. IEEE, Piscataway, N.J. CD-ROM.